JOURNAL OF CATALYSIS 148, 341–347 (1994)

Structure of SiO_2 on Al_2O_3 Monolayer Catalysts: Investigation by Infrared Spectroscopy and ^{29}Si MAS NMR

T.-C. Sheng,* S. Lang,† B. A. Morrow,† and I. D. Gay‡

*Department of Chemistry, Shandong University, Jinan, Shandong 250100, China; †Department of Chemistry, University of Ottawa, Ottawa, Ontario K1N 6N5, Canada; and ‡Department of Chemistry, Simon Fraser University, Burnaby, British Columbia V5A 1S6, Canada

Received September 14, 1993; revised March 1, 1994

Infrared spectroscopy and ^{29}Si MAS NMR are used to probe the structure of SiO_2 on Al_2O_3 catalysts prepared by chemical vapour deposition of $Si(OCH_3)_4$. SiO_2 loadings from about 0.2–2.5 statistical monolayers are studied. Infrared shows a gradual disappearance of AlOH vibrations and their replacement by SiOH vibrations as the SiO_2 loading is increased. A population of inaccessible AlOH is also observed. The Si–O–X asymmetric stretching frequency shows a continuous variation with SiO_2 content, consistent with X varying from Al at low levels to Si at high levels of silica. ^{29}Si NMR shows composite peaks at all SiO_2 levels. At the lowest level most intensity is concentrated in the -80 to -85 ppm range, corresponding to Si with attached –OAl groups. At the highest silica levels, the spectrum can be deconvoluted into peaks at -108, -100, and -92 ppm. These correspond to $Si(OSi)_4$, $Si(OSi)_3OH$, and mixtures of $Si(OSi)_2(OH)_2$ with –OAl-containing species. A model is proposed for build up of the silica layer on these catalysts. Random deposition of silica on any available surface is shown to give a semiquantitative account of the experimental results.

INTRODUCTION

Silica on alumina monolayer catalysts can be prepared by reaction of alumina with a silicon alkoxide at temperatures of a few hundred degrees Celsius (1–4). Like more traditional silica–alumina catalysts, these monolayer catalysts contain both Brønsted and Lewis acid sites on their surface. The numbers of these sites can be manipulated by varying the silica level and the conditions of preparation. Thus they present the possibility of preparing acidic surfaces with tailored characteristics.

In a previous paper (4) we have shown how the concentration of acid sites on these catalysts can be measured by ^{31}P NMR of adsorbed trimethyl phopshine. In the present paper we apply ^{29}Si NMR and FTIR spectroscopy to gain further insight into the structure of these catalysts.

EXPERIMENTAL

Samples of monolayer catalysts of varying SiO_2 levels were taken from the same batches used in our previous investigation (4), where the preparation is described. FTIR measurements were made on pressed disks of 7–10 mg/cm^2 density using a Bomem Michelson MB-100 instrument at a resolution of 4 cm^{-1}. Samples were degassed *in situ* in the IR cell at various temperatures, as described below. ^{29}Si MAS NMR measurements were made at 29.67 MHz on the instrument previously described (4). The same samples were used as in (4), i.e., samples with adsorbed trimethylphosphine. Since we did not observe any changes in the ^{29}Si spectrum for a 10-fold change in adsorbed TMP level, from 0.05 to 0.5 monolayers, the presence of the latter is unimportant. In all cases the ^{29}Si spectra were obtained by cross-polarization from surface protons, normally with a contact time of 4 ms. A proton-decoupling field of 38 kHz was used throughout, and a repolarization delay of 1 s, which gave an optimum signal-to-noise ratio. Magic angle spinning was used at rates between 1.6 and 2.4 kHz. No spectral changes were observed over this range. Cross-polarization is necessary because the samples are sealed in glass tubes, whose ^{29}Si signal is excessively intense if 90° pulse excitation is used. (Sato *et al.* (3) claim to have used 90° pulses for similar studies, using samples sealed in glass, and their spectra do not show glass resonances. We are unable to reproduce this result.)

RESULTS AND DISCUSSION

Infrared

Figure 1 shows the hydroxyl stretching region for silica on alumina samples, and for pure alumina, after vacuum activation at 400°C. The spectrum of γ-Al_2O_3 is entirely

0021-9517/94 $6.00

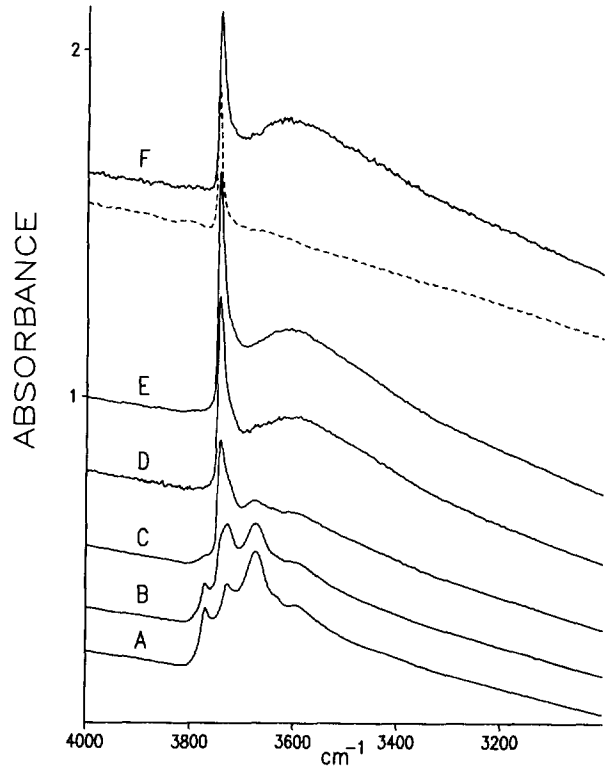

FIG. 1. (A) Infrared spectrum of pure alumina in the OH stretching region after vacuum activation at 400°C. (B–F) IR spectra of silica-on-alumina catalysts after vacuum activation at 400°C, the silicon loadings per square nanometer being (B) 1.3, (C) 4.2, (D) 8.2, (E) 12.3, and (F) 17.5. Curve (----) corresponds to the sample shown in (F) but after additional vacuum activation at 700°C. Each disk contained 7 mg/cm^2 of sample.

normal (5), having peaks at 3773, 3730, 3678, and 3600 cm^{-1}, with a shoulder at 3795 cm^{-1}. As silica is added, a new band appears at 3744 cm^{-1} due to isolated free silanol [SiOH or Si(OH)$_2$] stretching vibrations (6); this band appears as a shoulder at the lowest silica level. With increasing silica content this band grows and the AlOH bands progressively disappear, becoming invisible as distinct features at or above 12.3 SiO$_2$/nm^2.

At the higher silica coverages a broad band near 3610 cm^{-1} emerges as a distinct feature. This band has a considerable thermal stability insofar as it can only be removed by evacuation at 700°C (Fig. 1). Further, it was by and large not exchanged with D_2O at room temperature whereas the isolated silanol peak at 3744 cm^{-1} was almost completely exchanged, being displaced to 2760 cm^{-1}. Pure silicas which have been degassed at room temperature or 150°C usually exhibit broad IR bands near 3520 cm^{-1} due to H-bonded silanols and near 3650 cm^{-1} due to inaccessible silanols perturbed by interparticle contact (7). The latter only partially exchange with D_2O at room temperature and they can only be eliminated by evacuation at about 450°C. The alumina after 400°C activation also exhibits a broad feature at 3600 cm^{-1} which disappears after evacuation at 500°C, and this peak also resists exchange with D_2O at room temperature. Therefore, the broad 3610-cm^{-1} feature in the present study is undoubtedly due to a perturbed and relatively inaccessible SiOH or AlOH species (7, 8). However, this broad feature was also present after the initial deposition of Si(OMe)$_4$ and before the calcination to generate SiOH (see Fig. 2 for the case of a silica content of 15 Si/nm^2), and we speculate that this feature is mainly due to AlOH groups which have been rendered inaccessible because of the silica deposition.

Self-supporting alumina disks are opaque to IR radiation below about 1000 cm^{-1} due to strong absorption by the bulk Al–O–Al modes; for silica the cutoff in transmission is about 1300 cm^{-1} (9). However, if 0.1–0.3 mg of Si/cm^2 is dispersed in KBr or is deposited as a thin film on an optically transparent disk, the antisymmetric Si–O–Si vibration can be seen as a broad peak centered near 1100 cm^{-1}, asymmetric to high wave numbers (9). In zeolites of varying silica-to-alumina ratios (10) and glassy aluminosilicate minerals (11), the equivalent Si–O–Si or Si–O–Al

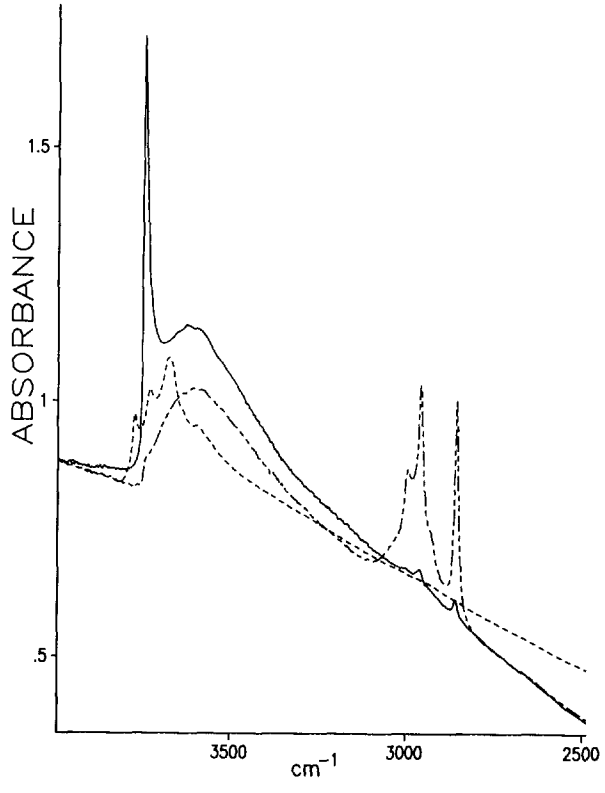

FIG. 2. IR spectrum of Al_2O_3 after activation at 400°C (------); after treatment of previous sample with Si(OMe)$_4$ so as to deposit 15 Si/nm^2 and before calcination, so that the surface is covered with SiOCH$_3$ groups (——, – –); and after calcining the previous sample in air at 500°C, followed by vacuum activation at 400°C (——).

vibration appears in the range between 1100 and 1000 cm^{-1}, it being lowest (about 1000 cm^{-1}) for zeolite A and for kalsylite, where the Si/Al ratios are one. For other zeolites, higher frequencies in this range can be correlated with a greater silica content and a greater number of Si–O–Si linkages (10).

Figure 3 shows IR spectra of the various samples dispersed in KBr disks, and Table 1 lists the wave number of the peak maximum between 1100 and 1000 cm^{-1}. It can be seen that there is a continuous shift of the position of the maximum to higher wave number with increasing Si deposition. This probably indicates that there is a statistical deposition of Si over the surface rather than a monolayer film initially; in the latter case one would expect Si–O–Al frequencies nearer the value of 1000 cm^{-1} found for zeolite A for all coverages up to the monolayer value. Most silicas contain about 7–8 Si atoms/nm^2 (12), and if all of these Si atoms up to our 8.2 Si/nm^2 level were uniformly deposited over the entire alumina surface, we might expect the peak wave number to be near 1000 cm^{-1}

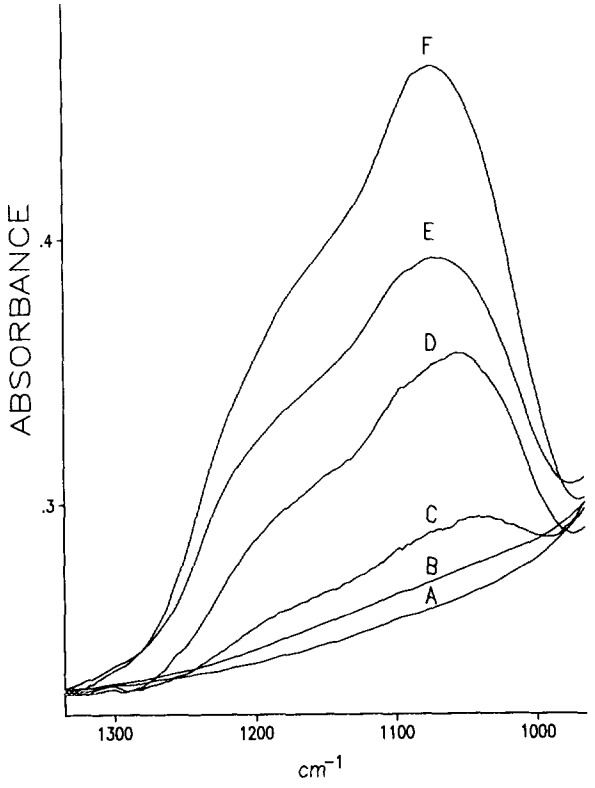

FIG. 3. IR spectra of catalysts in KBr disks in the spectral region associated with the SiOSi and SiOAl stretching modes. Samples (A–F) are the same as in Fig. 1, i.e., curve (A) is for pure Al_2O_3 and curve (F) is for the sample containing 17.5 Si/nm^2. The absorbance scale applies to curve (F), and the other curves have been normalized so that the absorptions due to bulk Al_2O_3 below 900 cm^{-1} (not shown) have approximately the same intensity. Peak maxima are reported in Table 1, except for curves (A) and (B), where no distinct maxima can be discerned.

TABLE 1

Si–O–Si Vibrational Peak Position

SiO_2/nm^2	Peak position (cm^{-1})
1.3	(No distinct peak)
4.2	1040
8.2	1057
12.3	1072
17.5	1077
SiO_2 gel	1092

rather than at 1057 cm^{-1}. Therefore some SiO_2 clustering occurs, even at the lower Si loadings.

At the higher loadings, the peak position is close to that expected for pure silica (6, 7, 13); clustering is probably quite extensive at this stage. Our previous study showed that there was still, even for the Si 17.5 sample, a significant number of Brønsted and Lewis acid sites. Thus, some of the original surface Al sites must still be accessible to PMe_3. Nonetheless, we conclude that AlOH is gradually replaced by Al–O–SiOH or Al–O–$(SiO)_n$–SiOH groups. IR alone cannot tell us whether the initial product might be species such as $(AlO)_3SiOH$ or $(AlO)_2Si(OH)_2$.

^{29}Si NMR

The ^{29}Si NMR spectra of the various samples are shown in Fig. 4. As can be seen there is a single peak whose maximum shifts from −85 to −101 ppm as the SiO_2 level increases. In all cases the peak appears to be composite. An expanded plot for the higher SiO_2 levels shows in addition to the main peak near −100 ppm a subsidiary peak near −92 ppm and some substantial intensity near −110 ppm. These spectra are qualitatively similar to those found by Sato *et al.* (3). At the three highest silica loadings, the spectra can be satisfactorily fitted as a superposition of three Gaussian peaks, but not by a smaller number. Figure 5 shows such a fit for the 12.3 SiO_2/nm^2 sample. The results of this fitting are collected in Table 2 for the three highest silica levels. Figure 5 also shows residual plots indicating that a two-peak model, or a three-peak model with parameters significantly different from those in Table 2, will not adequately represent the data. As can be seen, there is a gratifying agreement among the positions of the fitted peaks for the various samples. In all of the fits, amplitude, width, and position of the three components were treated as free parameters. The spectra at 1.3 and 4.2 SiO_2/nm^2 cannot be well represented by a similarly small number of peaks and must contain a more diverse range of surface species.

The chemical shift of ^{29}Si in aluminosilicate systems has been much studied in zeolites and natural minerals. The silicon shift is determined primarily by the groups to

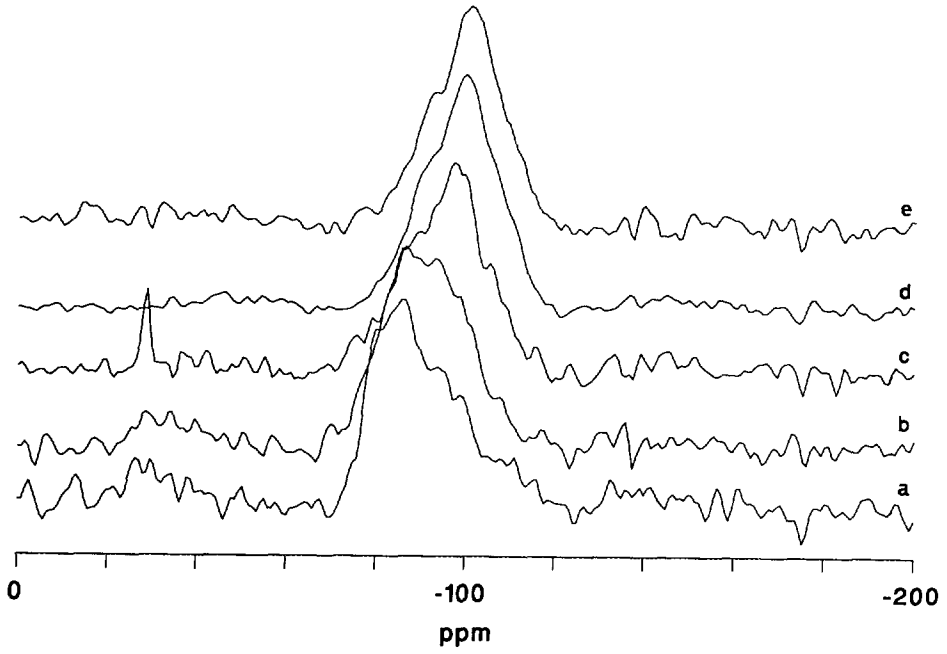

FIG. 4. ^{29}Si NMR spectra of catalysts with (a) 1.3, (b) 4.2, (c) 8.2, (d) 12.3, and (e) 17.5 SiO_2/nm^2.

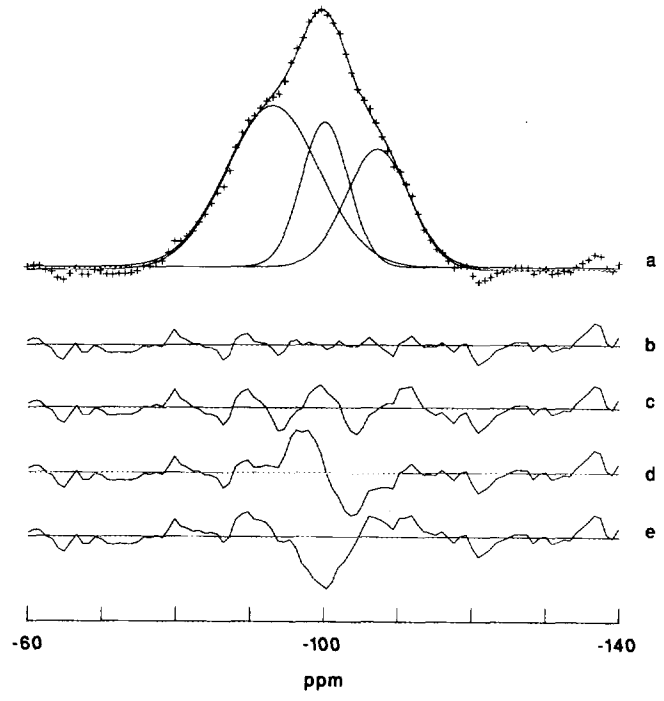

FIG. 5. (a) Gaussian fit to ^{29}Si spectrum of 12.3 SiO_2/nm^2 sample; crosses, experimental points, curves, Gaussian functions used to fit data, and their sum. (b) Residual plot of the fit shown in (a). (c–e) Residual plots from modified fitting models: (c) best fit with two Gaussians; (d) three-Gaussian fit with parameters as for (a) but with the central peak displaced 1 ppm to lower frequency; (e) as for (a) but with central peak increased in relative amplitude to comprise 30% of the total area. The residual plots have a vertical scale 1.5 times larger than plot (a).

which it is bonded. In oxide systems such as the present, these will be –OSi, –OAl, or –OH. The general silicon environment will thus be $Si(OSi)_n(OAl)_m(OH)_{4-n-m}$. Hereinafter we abbreviate this as S_nA_m, e.g., we use S_2A to represent $Si(OSi)_2(OAl)(OH)$.

Several studies of faujasite zeolites (14, 15) have shown a regular series of peaks for S_4, S_3A, S_2A_2, SA_3, and A_4 at typical shifts of -107, -101, -96, -90, and -84 ppm, respectively. It is found that the peaks can vary a few parts per million with the Si/Al ratio in the zeolite (16, 17) and with the nature of the cations (18). Similar trends are seen in other zeolites such as pentasils and mordenites (19), but the shifts are often several parts per million to lower frequency than found with faujasites. For zeolites of very low aluminum content, where S_4 is the dominant structural unit, it is often possible to resolve peaks from S_4 in different crystallographic environments (20, 21, 22). The shifts typically range from -106 to -116

TABLE 2

Gaussian Fits of ^{29}Si NMR Spectra[a]

SiO_2/nm^2	Peak 1	Peak 2	Peak 3
8.2	−92 (70)	−100 (20)	−108 (10)
12.3	−93 (51)	−100 (24)	−107 (25)
17.5	−92 (31)	−100 (36)	−108 (33)

[a] The first number in each column is the chemical shift of the Gaussian component in ppm, the number in parenthesis is the percentage of the total area in the component.

ppm. This range must reflect structural rather than chemical differences in the silicon environment. A correlation with the Si–O–Si angle has been proposed (22), and Janes and Oldfield (23) have shown that a wide range of aluminosilicate chemical shifts can be accounted for by a correlation involving both group electronegativity of substituents and Si–O–Si angle.

Chemical shifts involving OH groups are not as well established. On the surface of silica gel S_4, S_3, and S_2 are observed (24) to resonate at -109, -100, and -91 ppm, respectively. The same resonances are observed (25) on amorphous pyrogenic silica. In the mineral imogolite, A_3 is found to resonate at -78 ppm (26). If the Si–O–Si angle is taken to be 145.3°, which gives the value of -109 ppm for S_4, then the Janes–Oldfield correlation predicts -99 ppm for S_3, -89 ppm for S_2, and -81 ppm for A_3, in reasonable agreement with the above experimental values. Predicted values for S_2A and SA_2 are -93 and -87 ppm. Others have argued (27, 28) that S_2A resonates in the range of -83 to -87 ppm, SA_2 from -80 to -85 ppm, and A_3 at more positive shifts than -80 ppm.

In assessing these NMR spectra, it is important to consider what groups might be visible by cross-polarization. Cross-polarization depends on the H–Si dipolar coupling and will not be important if this coupling is small compared to the reciprocal of the contact time (30). (Unfavourable rotating-frame relaxation times will make cross-polarization still less successful.) Thus, for our standard 4-ms contact time we would not expect much signal from systems in which the dipolar coupling is less than 250 Hz. Using normal bond lengths and angles, the H–Si distance in a Si–O–H group is about 2.1 Å, giving a coupling of 2.5 kHz. For Si–O–Si–O–H the distance between H and the farther Si is about 3.6 Å in the most favourable configuration and 5.1 Å in the least. These distances correspond to diplar couplings of 520 and 180 Hz, respectively. Thus we should expect some signal from such a silicon, but it will be less strongly polarized than Si–O–H. Because of the inverse cube dependence of dipolar coupling on distance, we should not see significant signal from more distant Si–H configurations. In general one would expect H to be mainly present on the outer surface of the catalysts, as Al–O–H or Si–O–H.

Because of the many chemical and structural factors leading to small changes in ^{29}Si shifts, it is only possible to interpret the present results in broad terms. One might imagine that the first species visible by cross-polarization as SiO_2 is deposited on Al_2O_3 would be A_3. As noted above, this probably resonates above -80 ppm. Figure 4 shows no peak in this region, but at the lowest coverages it is clear that the tail of the peak has substantial intensity here. The centre of the peak is more likely to be SA_2 and/or S_2A. An alternative initial product might be A_2. The Janes–Oldfield correlation predicts -77 ppm for this species, and regardless of the absolute accuracy of this correlation, it probably does resonate at higher frequency than A_3, thus fitting less well with the experimental results. As coverage increases, there is a clear growth of intensity in the range of -90 to -93 ppm. This shift corresponds to S_2 or SA_3. The former will be a much better cross-polarizer, but on silica surfaces it is present only in relatively small amounts. On the other hand, the presence of SA_3 implies the buildup of a second layer of silica.

As noted above, the spectrum at 8.2 SiO_2/nm^2 and above is a superposition of three peaks, at -92, -100, and -108 ppm. As SiO_2 content increases, the latter two become increasingly larger in comparison with the former. They are thus likely to be peaks that do not involve Al–O–Si groupings. Given known chemical shift data the peak at -108 ppm is certainly S_4 and that at -100 ppm is most probably S_3. The peak at -92 ppm might be any of S_2, S_2A, SA_3, or a mixture of these.

Silica Buildup Model

Niwa *et al.* (1) took the view that silica first deposits to form a nearly complete monolayer on the substrate, amounting to 95% coverage at about 12 SiO_2/nm^2, with the last 5% of the substrate remaining uncovered at still higher silica loadings. There are several arguments against this proposal. First, it is more likely (12) that a silica monolayer contains 7–8 SiO_2/nm^2. Second, our ^{29}Si NMR spectra show intensity at -108 ppm, which can only be S_4, at coverages as low as 8.2 SiO_2/nm^2. It is difficult to see how S_4 can be present unless there are regions with at least a three-layer buildup of SiO_2. Third, the low-frequency IR results show that there is a progressive increase in the number of Si–O–Si linkages as the Si loading increases; for the monolayer model (1) up to 12 SiO_2/nm^2 we would expect a growth in the intensity of the Si–O–Al band near 1010–1040 cm^{-1} on increasing silica loading but no shift of the peak maximum to a higher wave number. Finally Niwa *et al.* offer no explanation as to why about 5% of the alumina remains uncovered. We are in agreement on the experimental point; our ^{31}P NMR (4) results show that at 17.5 SiO_2/nm^2 about 6% of the original Lewis sites of the alumina remain.

The main features of the above experimental results can be explained by a simple model in which SiO_2 is deposited at random on whatever surface is available. We treat this as a problem of deposition of successive silica layers, realizing that this is probably an oversimplification.

Using Θ_1 to represent the fraction of alumina substrate covered by one or more layers of silica, we assume random deposition and write

$$\frac{d\Theta_1}{dn} = k(1 - \Theta_1), \qquad (1)$$

where n is the amount of silica deposited per square nanometer and k is the reciprocal of the silica loading required for one layer. Similarly using Θ_2 for the fraction covered by two or more layers of silica, we write

$$\frac{d\Theta_2}{dn} = k(\Theta_1 - \Theta_2), \tag{2}$$

with similar equations for Θ_3, etc. We define Φ_1 to be the fraction of the surface covered by *exactly* one layer of silica; $\Phi_1 = \Theta_1 - \Theta_2$, with similar equations for Φ_2, etc. The Φ_i then obey the differential equations

$$\frac{d\Phi_0}{dn} = -k\Phi_0 \tag{3}$$

and

$$\frac{d\Phi_i}{dn} = k(\Phi_{(i-1)} - \Phi_i), \quad i > 0. \tag{4}$$

The solution to these equations is

$$\Phi_i = \frac{(kn)^i}{i!}e^{-kn}. \tag{5}$$

Figure 6 shows a plot of Φ_0 to Φ_5 for the relevant range of silica levels, using a k value of 0.143 nm^2. This value was chosen as the reciprocal of the approximate silica content in a single layer, 7 nm^{-2} (12). As can be seen, this value gives 8% of bare substrate at our highest silica loading, in good agreement with the 6% residual Lewis sites found in (4).

This model permits some predictions to be made about relative abundances of various surface species, since this depends on what layers are present. We assume that the outermost layer is largely hydroxylated, consistent with the infrared results above. The first deposited silica layer adjacent to the alumina would be expected to contain Si with at least one Al–O–Si bond. Species such as A_3 and A_2 would be expected to form first, and these might gradually be converted to A_2S, AS_2, and AS as the silicon density in the first layer increases. When the second layer begins to form, first-layer species could be converted to hydroxyl-free species such as A_3S, A_2S_2, and perhaps AS_3. In addition the second layer can contain the Al-free species S_3 and S_2. Finally, only with the deposition of the third and subsequent layers would the fully silicated S_4 species be expected in appreciable amounts.

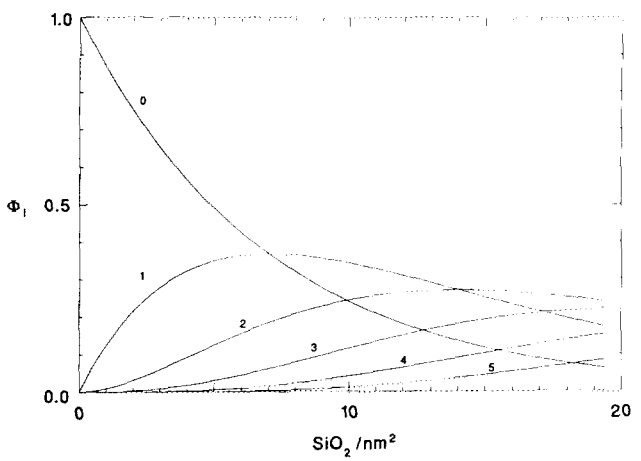

FIG. 6. The functions Φ_i, $i = 0, \ldots, 5$, computed with a k value of 0.143 nm^2.

In order to make a comparison with the ^{29}Si NMR results, we must take into account the distance dependence of cross-polarization efficiency, as discussed above. This is difficult to do in a rigorous manner. We therefore oversimplify the problem by assuming that Si in the two outermost layers of the deposit is visible by CP NMR (by cross-polarization from surface OH) and that Si more deeply buried is invisible, due to greater distance from protons. Thus, the fraction of NMR-visible Si in the first layer is taken to be $\Phi_1 + \Phi_2$, that in the second layer to be $\Phi_2 + \Phi_3$, etc. So the total visible Si in the deposit is given by $\Phi_1 + 2\Phi_2 + 2\Phi_3 + \ldots$.

S_4 can be expected to be present when three or more layers of silica have been deposited, and in terms of the present model its visible relative amount is given by $\Phi_3 + \Phi_4 + \ldots$. From the calculations of Fig. 6 we find the fraction of visible Si present as S_4 to be 0.11, 0.19, and 0.28 respectively for the 8.2-, 12.3-, and 17.5-nm^{-2} samples. This is in reasonable agreement with the ^{29}Si NMR results, which give 0.10, 0.25, and 0.33 respectively for the intensity fractions in the −108-ppm peaks of these samples.

We can proceed in a similar manner to compare the intensity of the −100-ppm peak with the amount of S_3 predicted by our model. Assuming the first layer to consist of species involving Al, S_3 and S_2 will be found in layers two and above when these are not covered by subsequent layers. The sum of S_3 and S_2 will thus be given by $\Phi_2 + \Phi_3 + \Phi_4 + \ldots$. Based on previous literature for the relative abundance of these species on silica (25, 31) we assume that 80% of this total is S_3. The model then predicts visible S_3 fractions 0.26, 0.31, and 0.35 for the above three samples, compared with the NMR intensity fractions of 0.20, 0.24, and 0.36 in the -100-ppm peak. It thus appears that our simple model of Si deposition accounts very well for the main features of the NMR results, bearing in mind the uncertainties arising from cross-polarization efficiencies.

Thus we find that both the infrared and the NMR results support a model of random silica deposition. Although the former are qualitative and the latter only semiquantitative,

due to uncertainties in cross-polarization efficiencies, both sets of data are in contradiction to what would be expected for a model in which silica builds up one monolayer at a time.

ACKNOWLEDGMENTS

This research was supported by grants from the Natural Sciences and Engineering Research Council of Canada, from Imperial Oil Ltd., and from the Dean of Science, Simon Fraser University.

REFERENCES

1. Niwa, M., Katada, N., and Murakami, Y., *J. Phys. Chem.* **94,** 6441 (1990).
2. Sato, S., Toita, M., Sodesawa, T., and Nozaki, F., *Appl. Catal.* **62,** 73 (1990).
3. Sato, S., Sodesawa, T., Nozaki, F., and Shoji, H., *J. Mol. Catal.* **66,** 343 (1991).
4. Sheng, T.-C. and Gay, I. D., *J. Catal.* **145,** 10 (1944).
5. Knözinger, H., and Ratnasamy, P., *Catal. Rev. Sci. Eng.* **17,** 34 (1978); Knözinger, H., and Boehm, H. P., *Catal. Sci. Technol.* (J. R. Anderson and M. Boudart, Eds.), Vol. 4 p. 40. Springer-Verlag, Berlin, 1983.
6. Morrow, B. A., and McFarlan, A. J., *J. Phys. Chem.* **96,** 1395 (1992).
7. Morrow, B. A., and McFarlan, A. J., *Langmuir* **7,** 1695 (1991), and refs. therein.
8. Zecchina, A., Bordiga, S., Spoto, G., Marchese, L., Petrini, G., Leefanti, G., and Padovan, M., *J. Phys. Chem.* **96,** 4985, 4991 (1992).
9. Morrow, B. A., *in* "Spectroscopic Studies of Heterogeneous Catalysis" (J. L. G. Fierro, Ed.). Elsevier, Amsterdam, 1990. Studies in Surface Science and Catalysis, Vol 57A, p. A161.
10. Flanigen, E. M., *in* "Zeolite Chemistry and Catalysis" (J. A. Rabo, Ed.), ACS Monograph Series, Vol 171, p. 80. American Chemical Society, Washington, DC, 1976.
11. Handke, M., and Mozgawa, W., *Vibr. Spectrosc.* **5,** 75 (1993).
12. Berendsen, G. E., and de Galan, L., *J. Liq. Chromatogr.* **1,** 403 (1978).
13. Burneau, A., Barrès, O., Gallas, J. P., and Lavelley, J. C., *Langmuir* **6,** 1364 (1990); **7** 1235 (1991).
14. Lippmaa, E., Mägi, M., Samoson, A., Tarmak, M., and Engelhardt, G., *J. Am. Chem. Soc.* **103,** 4992 (1981).
15. Klinowski, J., Thomas, J. M., Fyfe, C. A., and Gobbi, G. C., *Nature* (London) **296,** 533 (1982).
16. Engelhartd, G., Lohse, U., Lippmaa, E., Tarmak, M., and Mägi, M., *Z. Anorg. Allg. Chem.* **482,** 49 (1981).
17. Klinowski, J., Ramdas, S., Thomas, J. M., Fyfe, C. A., and Hartman, J. S., *J. Chem. Soc. Faraday Trans. 2* **78,** 1025 (1982).
18. Thomas, J. M., Fyfe, C. A., Ramdas, S., Klinowski, J., and Gobbi, G. C., *J. Phys. Chem.* **86,** 3061 (1982).
19. Nagy, J. B., Gabelica, Z., Debras, G., Bodart, P., and Derouane, E. G., *J. Mol. Catal.* **20,** 327 (1983).
20. Fyfe, C. A., Gobbi, G. C., Klinowski, J., Thomas, J. M., and Ramdas, S., *Nature* (London) **296,** 530 (1982).
21. Nagy, J. B., Gabelica, Z., Derouane, E. G., and Jacobs, P. A. *Chem. Lett.*, 2003 (1982).
22. Thomas, J. M., Klinowski, J., Ramdas, S., Hunter, B. K., and Tennakoon, D. T. B., *Chem. Phys. Lett.* **102,** 158 (1983).
23. Janes, N., and Oldfield, E., *J. Am. Chem. Soc.* **107,** 6769 (1985).
24. Maciel, G. E., and Sindorf, D. W., *J. Am. Chem. Soc.* **102,** 7607 (1980).
25. Morrow, B. A., and Gay, I. D., *J. Phys. Chem.* **92,** 5569 (1988).
26. Barron, P. F., Wilson, M. A., Campbell, A. S., and Frost, R. L., *Nature* (London) **299,** 616 (1982).
27. Kirkpatrick, R. J., Smith, K. A., Schramm, S., Turner, G., and Yang, W.-H., *Ann. Rev. Earth Planet. Sci.* **13,** 29 (1985).
28. Fitzgerald, J. J., Murali, C., Nebo, C. O., and Fuerstenau, M. C., *J. Colloid Interface Sci.* **151,** 229 (1992).
29. Deleted in proof.
30. Wu, X., and Zilm, K. L., *Magn. Reson.* **102,** 205 (1993).
31. McFarlan, A. J., and Morrow, B. A., *J. Phys. Chem.* **95,** 5388 (1991).